INDIAN JOURNAL OF SCIENCE AND TECHNOLOGY

RESEARCH ARTICLE

Flow Characteristics of Casson Nanofluid Over a Moving Wedge

Prashant Sutkar[1]*

1 Assistant Professor, Department of Mathematics and Applied Mathematics, Science College, Nanded, 431606, Maharashtra, India

OPEN ACCESS

Received: 30-01-2024

Accepted: 29-02-2024

Published: 28-03-2024

Citation: Sutkar P (2024) Flow Characteristics of Casson Nanofluid Over a Moving Wedge. Indian Journal of Science and Technology 17(13): 1349-1356. https://doi.org/10.17485/IJST/v17i13.234

* **Corresponding author**.

prashantsutkar@gmail.com

Funding: None

Competing Interests: None

Published By Indian Society for Education and Environment (iSee)

ISSN
Print: 0974-6846
Electronic: 0974-5645

Abstract

Objectives: Analysis of Cassion nanofluid over a wedge is carried out for magnetohydrodynamics (MHD), wedge parameter, thermal radiation parameter, non-uniform heat source or sink and suction/injection parameter. **Method:** With the help of similarity transformations, the governing partial differential equations corresponding to the momentum and heat transfer are reduced to a set of non-linear ordinary differential equations. Numerical solutions of these equations are obtained. **Findings:** The influence of relevant parameters on non-dimensional velocity and temperature profiles are depicted graphically and in table form for two flow cases namely for nanofluid and for regular fluid. **Novelty:** It is experienced that with an escalation of magnetic field parameter, the flow is accelerated. Velocity profile shows growth with enhanced wedge parameter. Nusselt number and Skin friction parameters are discussed with the assistance of the table for base fluid and nanofluid.

Keywords: Nanofluid; Suction; Injection; MHD; Casson fluid; Wedge

1 Introduction

Casson fluid is first invented by Casson in 1959. It is based on the structure of liquid phase and interactive behaviour of solid, of a two-phase suspension. Some examples of Casson fluid are Jelly, honey, tomato sauce and concentrated fruit juices. When human red blood cells, fibrinogen, globulin in aqueous base plasma, protein, and other components are present, human blood can also be considered as a Casson fluid. Several scientists, engineers, mathematicians, and academics have studied Casson fluid flow in the context of fluid mechanics, depending on various circumstances.

Mishra and Kumar[(1)] have explored modeling and numerical simulation of hydromagnetic natural convection Casson fluid flow with n^{th}-order chemical reaction and Newtonian heating in porous medium, taking into account the various parameters on the flow properties of Casson fluid. Thameem and Sivara[(2)] studied stability analysis Casson fluid flow over a wedge. Shanmugapriya[(3)] discussed physical model for multiple slip flow of magnetized Casson nanofluid over a wedge. Anomitra and Pranithal[(4)] analyzed thermophoretic and Brownian effects. Suresh Kumar et al.[(5)] analyzed the flow, heat, and mass transfer behavior of Casson nanofluid past an exponentially stretching surface in presence of Hall current, thermal radiation, Brownian motion and thermophoresis. Radha[(6)] studied the effect/result of heat source

parameter over a wedge. Shah et al[7] examined the transfer of heat in magnetized Carreau fluid with chemical reaction and under influence of thermal radiation over nonlinear stretching/shrinking surface. The impact of thermophoretic particle deposition on heat and mass transfer throughout the dynamics of Casson fluid flow over a moving thin needle has been explored by Naveenkumar et al.[8]. Double diffusive convection and cross diffusion effects on the Casson fluid across a Lorentz force driven Riga plate in a porous medium with heat sink, was evaluated by Kanayo et al.[9]. Unsteady Magnetohydrodynamics oscillatory Casson fluid flow over an inclined vertical porous plate in the presence of Soret effects and chemical reaction with heat absorption has been explored by Raghunath and Obulesu[10]. An investigation of the micropolar nanofluid sandwiched between permeable fluids enclosed in a horizontal channel is illustrated by Umavathi et al.[11]. The investigation of MoS2-Sio2-Go/water ternary hybrid nanofluid containing motile gyrotactic microorganisms was carried by Mishra et al.[12]. Mishra et al.[13] developed machine learning algorithm to predict the heat transfer rate at the surface.

The hydro-thermal characteristics of two different types of hybrid nanofluid flow, namely MoS_2-SiO_2/water hybrid nanofluid and $MoS_2-SiO_2-GO/$ water ternary hybrid nanofluid flow toward an inclined cylinder in the presence of heat generation/absorption and viscous dissipation is analyzed by Mishra and Pathak[14]. Over an inclined cylinder the flow attributes of a carbon nanotube based hybrid nanofluid is studied by Mishra and Upreti[15]. Aspects of electroosmotics are analysed by Akbar NS and research group[16–18]. The study of elevated stretched cylinder and peristaltic flow is carried by Akbar et al.[19,20]. Double layered convective heated flow of Eyring Powell fluid across an elevated stretched cylinder using intelligent computing approach is analyzed by Akbar et al[21] in his study.

Boundary layers are developed over a continuous moving surface in the fluid region. They are significant in nature because they have an impact on transport phenomena. When temperature variations lead to variations in density, which in turn produce buoyancy forces that operate directly on the fluid's constituent parts, natural convection occurs inside the fluid. Over the past few decades, there has been a great deal of interest in the theoretical and practical investigation of heat transfer MHD free convection flow with thermal radiation effects on a vertical plate. Since magneto hydrodynamics flow and heat transfer over a continuous stretching sheet are used in many industrial manufacturing processes, including the production of paper, ceramic polymer extrusion, and plastic, they are considered to be among the most significant problems in fluid dynamics. Casson nanofluid flow is the topic of great interest of many researchers. Wedge used in several industrial applications one of which is to regulate fluid flow across the fluids path. While takeoff and landing of airplane the air flow is divided by a wedge or plate. The motivation behind this investigation is to better understand the behavior of nanofluid, in different flow scenarios and under the influence of magnetic fields. The novelty of this study lies in investigating mass and heat transmission rates in nanofluid. The findings highlight the complex interplay between these factors and their impact on the transport process. Keeping this fact in mind, an attempt is made to investigate the flow and heat transfer characteristics of Casson nanofluid in a case of moving wedge.

2 Methodology

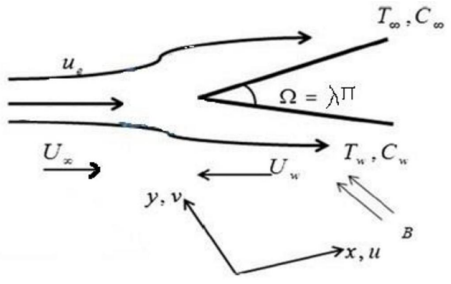

Fig 1. Flow geometry

We presumed magnetohydrodynamic two dimensional, time independent flow of nanoliquid along a poignant wedge as depicted in Figure 1. The wedge angle is given by $\Omega = \lambda\, pi$ where $\lambda = (2n/n+1)$ is wedge angle parameter. A variable magnetic field is applied along the flow direction as shown in Figure 1.

It is noted that the effect of thermophoresis is considered in the present analysis. The stretching and free stream velocity of the wedge is given by

$$u_w(x) = U_w x^n,\ u_e(x) = U_\infty x^n \tag{1}$$

Here T_w, T_∞, C_w and C_∞ are temperature and concentration at the boundary and free stream.

In view of the aforesaid physical presumptions the flow governing equations are given below.

$$u_x + v_y = 0 \tag{2}$$

$$u\left(u_x\right) + v\left(u_y\right) = u_e\left(u_e\right)_x + \frac{\mu_{hnf}}{\rho_{hnf}}\left(1+\beta^{-1}\right)\left(u_{yy}\right) - \frac{\sigma_{hnf}}{\rho_{hnf}}B_0^2(x)\left(u_e - u\right) \tag{3}$$

$$u\left(T_x\right) + v\left(T_y\right) = \frac{k\left(T_{yy}\right)}{\left(\rho c_p\right)_{nf}} + \frac{\left(16\sigma^* T_\infty^3\right)}{\left(3k^*\left(\rho c_p\right)_{nf}\right)}\left(T_{yy}\right) + q^{'''} \tag{4}$$

The respective boundary restrictions are

$$\left.\begin{array}{c} u = u_w(x), v = v_w(x), T = T_w, \ at\ y = 0, \\ u \to u_e, T \to T_\infty, \ as\ y \to \infty \end{array}\right\} \tag{5}$$

Where u and v are the velocity components. T is temperature. In order to transform the aforementioned Equations (2), (3), (4) and (5) to the dimensionless form we utilize the below similarity transformations,

$$\left.\begin{array}{c} \Psi = \left(2vxu_e/n+1\right)^{1/2} f(\eta), u = \Psi_y, v = -\Psi_x, \\ \eta = \left((n+1)u_e/2vx\right)^{1/2}, T = T_\infty + \theta(\eta)\left(T_w - T_\infty\right) \end{array}\right\} \tag{6}$$

In the energy Equation (6)

$$q''' = \left(k_f U_0/xv_f\right), \left\{A*\left(T_w - T_\infty\right)f' + B*\left(T - T_\infty\right)\right\} \tag{7}$$

is the irregular heat source/sink parameter, in which A^* and B^* are the coefficients of space and temperature dependent heat source and sink respectively. In order to transform the aforementioned Equation (2) is automatically satisfied using Equation (6) and Equations (3) and (4) transformed in dimensionless ODEs as follows

$$A_1 f^{''} + \lambda A_2 - \lambda A_2 f^{'2} + MA_3\left(f^{'} - 1\right) + A_2 f f^{''} = 0 \tag{8}$$

$$\left(1/Pr\right)\left(A_4 + 4R/3\right)\theta^{''} + A_5 f\theta^{'} + A^* f^{'} + B^*\theta = 0 \tag{9}$$

the transformed boundary restrictions are

$$\left.\begin{array}{c} f = S, f^{'} = \gamma, \theta = 1, \ at\ \eta = 0, \\ f^{'} = 1, \theta = 0, \ at\ \eta \to \infty, \end{array}\right\} \tag{10}$$

where $M, \lambda, \gamma, R, A^*, B^*, S$ and Pr are the dimensionless parameters magnetic field, wedge angle, wedge parameter, thermal radiation parameter, non-uniform heat source/sink, suction/injection, Prandtl number, respectively, they are defined as:

$$\left.\begin{array}{c} M = \left(2\sigma_f B_0^2/\rho_f U_\infty(n+1)\right), \lambda = \left(2n/(n+1)\right), \gamma = \left(U_w/U_\infty\right), \\ S = v_w(x)(n+1(vu_e(x))/2x)^{\frac{-1}{2}}, Pr = \left(\left(\mu c_p\right)_f/k_f\right), R = \left(4\sigma^* T_\infty^3/kk^*\right), \end{array}\right\} \tag{11}$$

The nanofluid restrictions are taken as,

$$\left.\begin{array}{l} A_1 = \dfrac{\mu_{nf}}{\mu_f} = (1-\phi)^{-2.5}, \\ A_2 = \dfrac{\rho_{nf}}{\rho_f} = (1-\phi) + \phi\dfrac{\rho_s}{\rho_f}, \\ A_3 = \dfrac{\sigma_{nf}}{\sigma_f} = \left[1 + \dfrac{3(\sigma-1)\phi}{(\sigma+2) - (\sigma-1)\phi}\right], \sigma = \dfrac{\sigma_s}{\sigma_f}, \\ A_4 = \dfrac{k_{nf}}{k_f} = \left(\dfrac{k_s + 2k_f - 2\phi k_f + 2\phi k_s}{k_s + 2k_f + 2\phi k_f - 2\phi k_s}\right), \\ A_5 = \dfrac{\left(\rho C_p\right)_{nf}}{\left(\rho C_p\right)_f} = 1 + \phi\dfrac{\left(\rho C_p\right)_s}{\left(\rho C_p\right)_f} \end{array}\right\} \tag{12}$$

Here, μ_{nf} represents the absolute viscosity and μ_f represent the viscosity of base fluid. The subscripts f and nf are respectively meant for base fluid and nanofluid. The physical entities of engineering interest are skin friction coefficient C_{fx}, and local Nusselt number Nu_x which are given as

$$\left.\begin{array}{c} Re_x^{0.5}\, C_{fx} = A_1 f''(0) \\ Re_x^{0.5}\, Nu_x = -\dfrac{(1+4R/3)}{(2/(n+1))^{0.5}} A_4 \theta'(0) \end{array}\right\} \tag{13}$$

The non-dimensional governing Equations (8) and (9) are solved using Runge-Kutta method with the help of boundary condition **11** (Equation (11)). The solutions are obtained by using similarity transformation for variation in magnetic field parameter, wedge parameter, thermal radiation parameter, suction /injection for velocity and temperature profiles.

3 Results and discussion

In order to analyze the results, numerical computation has been carried out for various values of the magnetic field parameter, wedge parameter, thermal radiation parameter, on-uniform heat source/sink and suction/injection. For illustration of the results, numerical values are plotted in Figure 2 through Figure 8. Effect of magnetic field parameter in the range $1 \leq M \leq 3$ on velocity and temperature with and without nanoparticles is highlighted with graphs in Figures 2 and 3 respectively in which temperature enhances. Figures 4 and 5 dissipates the effect of wedge parameter in the range from -0.3 to 0.3, on velocity and temperature with and without nanoparticles. The effect of thermal radiation parameter on temperature is highlighted in Figure 6 which shows growth for both base fluid and nanofluid. Figures 7 and 8 shows velocity profile for variation of non-uniform heat source/sink and suction/injection. Thermophysical properties of nanoparticle and base fluid is given in Table 1. Variation in Skin friction factor under various physical parameters for base fluid (Water) and nanofluid (Fe_3O_4-Water) cases is shown in Table 2. Skin friction factor for nanofluid have some higher values when compared with base fluid. Table 3 gives Variation in local Nusselt number under various physical parameters for base fluid (Water) and nanofluid (Fe_3O_4-Water) cases. Nusselt number for nanofluid suppresses in magnitude when compared with base fluid. Table 4 highlights the numerical values of skin friction parameter for variation in magnetic field, which shows similar results using different methods.

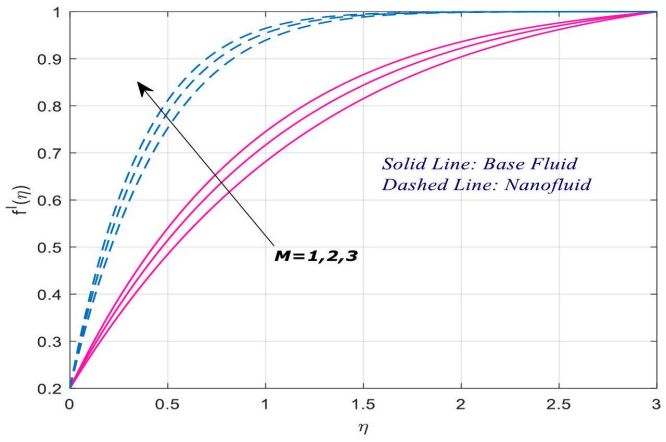

Fig 2. Effect of magnetic field parameter on velocity

Table 1. Thermophysical properties of nanoparticle and base fluids

Physical properties	Fe_3O_4	Water (Base fluid)
$C_p(J/kgK)$	670	4179
$\rho\,(kg/m^3)$	5180	997.3
$K(w/m)$	9.7	0.613
$\sigma(s/m)$	0.74×10^6	21

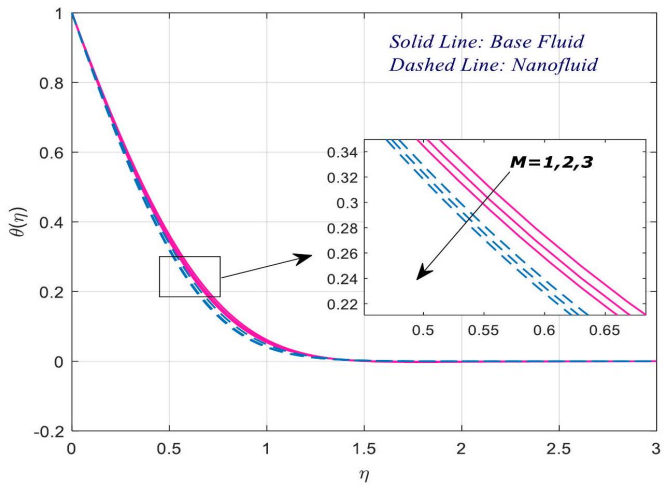

Fig 3. Effect of magnetic field parameter on temperature

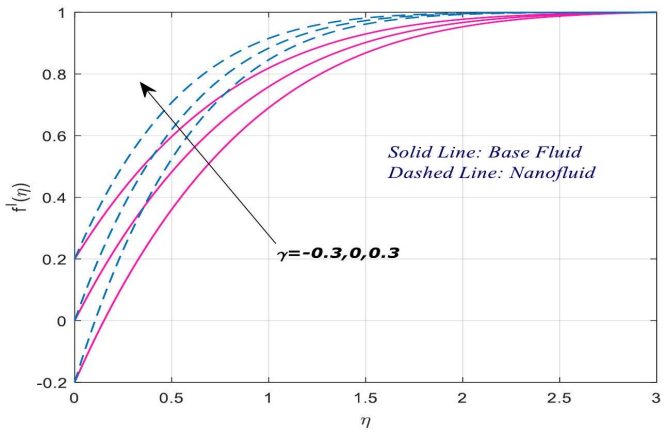

Fig 4. Effect of wedge parameter on velocity

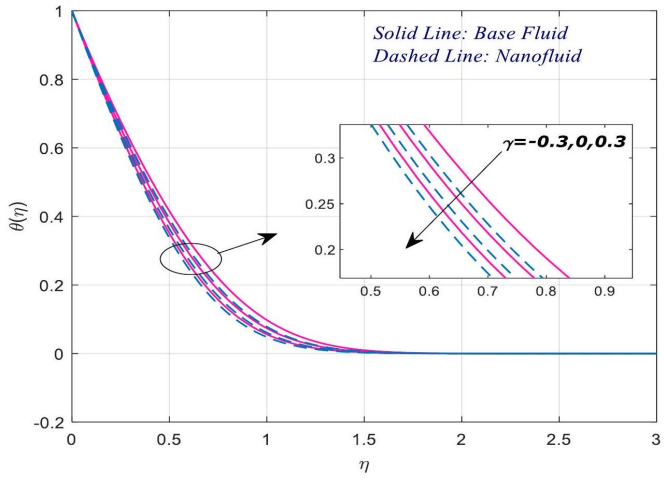

Fig 5. Effect of wedge parameter on temperature

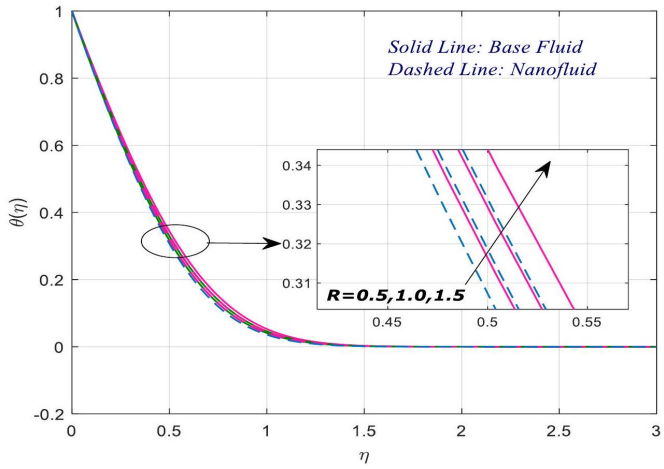

Fig 6. Effect of thermal radiation parameter on temperature

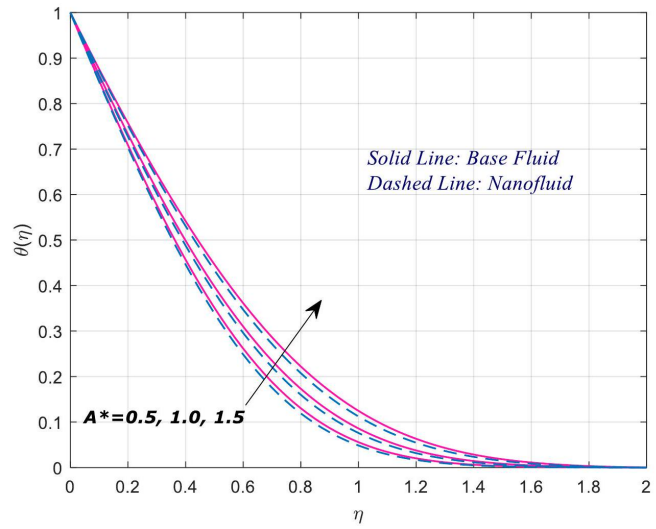

Fig 7. Variation of non-uniform heat source/sink

Table 2. Variation in Skin friction factor under various physical parameters for base fluid (Water) and nanofluid (Fe_3O_4-Water) cases

M	γ	ϕ	C_{fx}	
			Base fluid	**Nanofluid**
1			1.337063	1.879895
2			1.651684	2.108753
3			1.911372	2.313328
	-0.3		1.887266	2.622037
	0.0		1.622931	2.269244
	0.3		1.337063	1.879895
		0.01	1.539399	2.156715
		0.02	1.337063	1.879895
		0.03	1.174941	1.657140

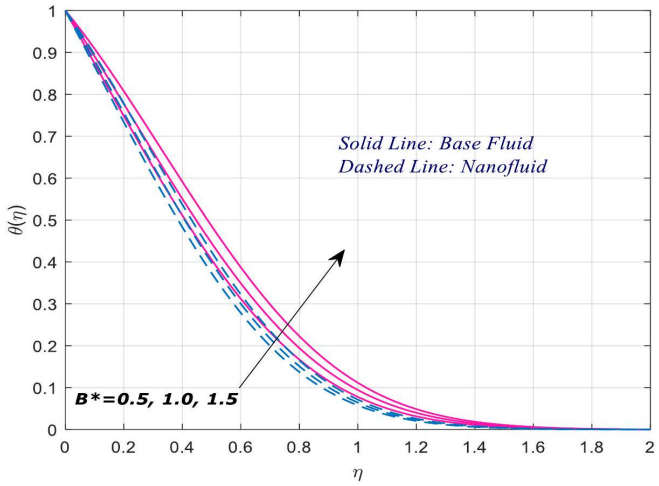

Fig 8. Profile for suction/injection

Table 3. Variation in local Nusselt number under various physical parameters for base fluid (Water) and nanofluid (Fe_3O_4-Water) cases

M	γ	R	A^*	B^*	Nu_x	
					Nanofluid	**Base fluid**
1					2.808875	1.983909
2					2.807506	1.984173
3					2.807078	1.984500
	-0.2				2.125250	1.521080
	0.0				2.482914	1.760646
	0.2				2.808875	1.983909
		1.0			3.313480	2.362174
		1.5			3.752140	2.690019
					4.147668	2.984620

Table 4. Authentication of obtained results forC_{fx} for various values of M

M	Shooting	KBM	Present results
0.3	1.352628	1.352628	1.3526285
0.6	1.373606	1.373606	1.3736062
0.9	1.385734	1.385734	1.3857347

4 Conclusions

Solution for the flow of a Casson nanofluid and heat transfer over a wedge is presented. A transformed set of equations is obtained and solved. With increase in magnetic field parameter, the fluid velocity is found to increase whereas temperature decreases. Increasing the value of wedge parameter improves the velocity profile and decreases the temperature. Skin friction parameter and Nusselt number have superior values for nanofluid when compared with base fluid. The same results are obtained for Skin friction parameter using different solution methods.

Nomenclature

θ -dimensionless temperature; ϕ -dimensionless concentration; f -dimensionless velocity; C_{fk} -skin friction coefficient; Nu_x -local Nusselt number; M -Magnetic field parameter; λ -wedge angle; γ -wedge parameter; R -thermal radiation parameter;

A^* -non-uniform heat source/sink; B^* -suction/injection; Pr -Prandtl number; C_p -specific heat at constant pressure $(J/kgK)x$ -distance along the surface; (m) ; y -distance normal to the surface (m); T -temperature of the fluid (K) ; C -concentration of the fluid (Moles $/kg$); (ρC_p) -heat capacity of the nanofluid$\left(kg/m^3K\right)$; $(\rho C_p)_x$ -effective heat capacity solid $\left(kg/m^3K\right)$; B_0 -magnetic induction parameter; η -similarity variable; u -velocity component; v -velocity component

References

1) Mishra A, Kumar M. Numerical analysis of MHD nanofluid flow over a wedge, including effects of viscous dissipation and heat generation/absorption, using Buongiorno model. *Heat Transfer*. 2021;50(8):8453–8474. Available from: https://doi.org/10.1002/htj.22284.
2) Basha T, Sivara H, R. Stability Analysis of Casson Nanofluid Flow over an Extending/Contracting Wedge and Stagnation Point. *Journal of Applied Computational Mechanics*. 2022;8(2):566–579. Available from: https://doi.org/10.22055/jacm.2020.32618.2045.
3) Shanmugapriya M, Sundareswaran R, Krishna SG, Alameri A. Investigation of Magnetized Casson Nanofluid Flow along Wedge: Gaussian Process Regression. *International Journal of Mathematics and Mathematical Sciences*. 2024;2024:1–24. Available from: https://doi.org/10.1155/2024/2880748.
4) Chakraborty A, Janapatla P. Study of Cassonnanofluid flow over a wedge with variable magnetic effect, thermal radiation, and melting effects. *Numerical Heat Transfer, Part B: Fundamentals* . 2023. Available from: https://doi.org/10.1080/10407790.2023.2266128.
5) Kumar YS, Hussain S, Raghunath K, Ali F, Guedri K, Elain SM, et al. Numerical analysis of magnetohydrodynamics Casson nanofluid flow with activation energy, Hall current and thermal radiation. *Scientific Reports*. 2023;13:1–19. Available from: https://doi.org/10.1038/s41598-023-28379-5.
6) Madhavi MR, Sridhar W, Nagesh P. Numerical investigations of MHD Casson nanofluid flow over a wedge through porous medium. In: ESSENCE OF MATHEMATICS IN ENGINEERING APPLICATIONS: EMEA-2020;vol. 2375, Issue 1 of AIP Conference Proceedings. AIP Publishing. 2021;p. 30011. Available from: https://doi.org/10.1063/5.0066944.
7) Shah SAGA, Hassan A, Karamti H, Alhushaybari A, Eldin SM, Galal AM. Effect of thermal radiation on convective heat transfer in MHD boundary layer Carreau fluid with chemical reaction. *Scientific Reports*. 2023;13(1):1–11. Available from: https://doi.org/10.1038/s41598-023-31151-4.
8) Kumar RN, Gowda RJP, Madhukesh JK, Prasannakumara BC, Ramesh GK. Impact of thermophoretic particle deposition on heat and mass transfer across the dynamics of Casson fluid flow over a moving thin needle. *Physica Scripta*. 2021;96(7):075210. Available from: https://iopscience.iop.org/article/10.1088/1402-4896/abf802#:~:text=In%20his%20study%20he%20reported,reducing%20factor%20of%20liquid%20flow.
9) Asogwa KK, Alsulami MD, Prasannakumara BC, Muhammad T. Double diffusive convection and cross diffusion effects on Casson fluid over a Lorentz force driven Riga plate in a porous medium with heat sink: An analytical approach. *International Communications in Heat and Mass Transfer*. 2022;131:105761. Available from: https://doi.org/10.1016/j.icheatmasstransfer.2021.105761.
10) Kodi R, Mopuri O. Unsteady MHD oscillatory Casson fluid flow past an inclined vertical porous plate in the presence of chemical reaction with heat absorption and Soret effects. *Heat Transfer*. 2022;51(1):733–752. Available from: https://doi.org/10.1002/htj.22327.
11) Umavathi JC, Sutkar PS. Amplification of Heat Transfer in Three Immiscible Fluids: Micropolar Nanofluid Encased with Porous Matrix. *Journal of Nanofluids*. 2023;12(4):1107–1118. Available from: https://doi.org/10.1166/jon.2023.1992.
12) Mishra A, Pathak G, Kumar A. Computational Analysis of Bioconvection of MoS2-SiO2-GO/H2O Ternary Hybrid Nanofluid Containing Gyrotactic Microorganisms over an Exponentially Stretching Sheet with Chemical Reaction. *BioNanoScience*. 2023. Available from: https://doi.org/10.1007/s12668-023-01279-8.
13) Mishra A, Rawat SK, Yaseen M, Pant M. Development of machine learning algorithm for assessment of heat transfer of ternary hybrid nanofluid flow towards three different geometries: Case of artificial neural network. *Heliyon*. 2023;9(11):1–36. Available from: https://doi.org/10.1016/j.heliyon.2023.e21453.
14) Mishra A, Pathak G. A comparative analysis of MoS2-SiO2/H2O hybrid nanofluid and MoS2-SiO2-GO/H2O ternary hybrid nanofluid over an inclined cylinder with heat generation/absorption. *Numerical Heat Transfer, Part A: Applications*. 2023. Available from: https://doi.org/10.1080/10407782.2023.2228483.
15) Mishra A, Upreti H. Computational analysis of radiative nanofluid flow past an inclined cylinder with slip effects using the Yamada–Ota model. *Numerical Heat Transfer, Part A: Applications*. 2023. Available from: https://doi.org/10.1080/10407782.2023.2258556.
16) Akram J, Akbar NS. Electroosmotically actuated peristaltic-ciliary flow of propylene glycol + water conveying titania nanoparticles. *Scientific Reports*. 2023;13(1):1–18. Available from: https://doi.org/10.1038/s41598-023-38820-4.
17) Akbar NS, Rafiq M, Muhammad T, Alghamdi M. Electro osmotically interactive biological study of thermally stratified micropolar nanofluid flow for Copper and Silver nanoparticles in a microchannel. *Scientific Reports*. 2024;14(1):1–15. Available from: https://doi.org/10.1038/s41598-023-51017-z.
18) Akbar NS, Muhammad T. Physical aspects of electro osmotically interactive Cilia propulsion on symmetric plus asymmetric conduit flow of couple stress fluid with thermal radiation and heat transfer. *Scientific Reports*. 2023;13(1):1–17. Available from: https://doi.org/10.1038/s41598-023-45595-1.
19) Ghailan KY, Akbar NS, Albakri A, Alshehri MM. Biological analysis of emerging nanoparticles with blood through propagating flow along a plumb porous canal in the occurrence of energy and heat transfer. *Surfaces and Interfaces*. 2023;40:103013. Available from: https://doi.org/10.1016/j.surfin.2023.103013.
20) Akbar NS, Mehrizi AA, Rafiq M, Habib MB, Muhammad T. Peristaltic flow analysis of thermal engineering nano model with effective thermal conductivity of different shape nanomaterials assessing variable fluid properties. *Alexandria Engineering Journal 2023*. 2023;81:395–404. Available from: https://doi.org/10.1016/j.aej.2023.09.027.
21) Alghamdi M, Akbar NS, Zamir T, Muhammad T. Double layered combined convective heated flow of Eyring-Powell fluid across an elevated stretched cylinder using intelligent computing approach. *Case Studies in Thermal Engineering*. 2024;54:1–21. Available from: https://doi.org/10.1016/j.csite.2024.104009.